Spectroscopy of highly charged tungsten ions with Electron Beam Ion Traps

SAKAUE A. Hiroyuki[1], KATO Daiji[1], MORITA Shigeru[a], MURAKAMI Izumi[1],
Yamamoto Norimasa[2], OHASHI Hayato[3], YATSURUGI Junji[3],
and NAKAMURA Nobuyuki[3]

[1]*National Institute for Fusion Science, Toki, Gifu 509-5292, JAPAN*
[2]*Chubu University, Kasugai, Aichi, 487-8501, JAPAN*
[3]*Institute for Laser Science, The University of Electro-Communications, Chofu, Tokyo 182-8585, JAPAN*

Abstract

We present spectra of highly charged tungsten ions in the extreme ultra-violet (EUV) by using electron beam ion traps. The electron energy dependence of spectra is investigated of electron energies from 490 to 1440 eV. Previously unreported lines are presented in the EUV range, and some of them are identified by comparing the wavelengths with theoretical calculations.

Keywords: Highly charged ions, Tungsten, EBIT.

1.Introduction

Tungsten will be used for the material of divertor plates in ITER because of higher threshold energies for sputtering by light ion bombardment, the highest melting point in the chemical elements, and less tritium retention than that in carbon based materials. However, since extremely high particle- and heat-fluxes of intermittent edge plasma transports (*e.g.* edge-localized-mode) in ITER would cause serious damages to such components, tungsten is considered to be one of the most abundant impurities in the ITER plasma. Emission lines of highly charged tungsten ions thus play an important role in the spectroscopic diagnostics of the ITER plasma, and consequently the spectroscopic data of tungsten ions have been studied at several facilities[1-3].

An electron beam ion trap is a useful device for the systematic spectroscopic studies of tungsten ions[4-7]. We have been using two kinds of EBIT; one of them is the high-energy EBIT (Tokyo-EBIT)[8] constructed at the University of Electro-Communications (UEC), and another is the low-energy compact EBIT (called "CoBIT")[9-11] developed for spectroscopic studies of moderate charge state ions. We

have constructed two CoBIT, and installed them at the UEC and National Institute for Fusion Science. The electron energy range of CoBIT and the Tokyo-EBIT is 0.1 - 2 keV and 2 - 200 keV, respectively, and the accessible charge states of tungsten are about 10 – 40 and 40 – 74, respectively. The complementary use of them thus enables us to acquire the atomic data of tungsten ions for almost the whole range of charge states. In this paper, we reported the data of CoBIT.

2.Experimental apparatus

In the present EBIT experiments, we used the low-energy compact EBIT. In the EBIT, an electron beam emitted from an electron gun is compressed with a pair of superconducting magnets. Since ions ionized by the electron beam are trapped by the electrostatic potential well in the axial direction and also by the electronic space charge potential in the radial direction, they can be successively ionized toward higher charge states. The parameters of CoBIT are listed in TABLE 1.

FIGURE 1 show the present experimental setup for CoBIT. CoBIT has six ports currently used for an EUV spectrometer, gas injector, pinhole camera, visible spectrometer and K-Cell injector. The EUV spectrometer is of a slit-less type especially designed for CoBIT. Since the trapped ions are excited by a thin electron beam, the EBIT represents a line source so that an entrance slit can be omitted. A laminar-type diffraction grating (1200 gr/mm or 2400 gr/mm depending on wavelength) is used to focus the radiation on the surface of a back illuminated CCD (PIXIS-XO:400B).

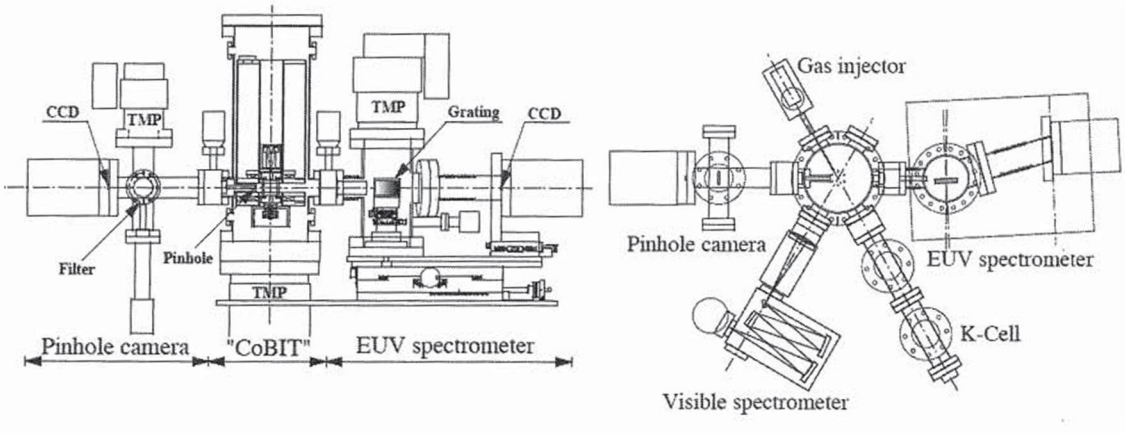

FIGURE 1. The experimental apparatuses of CoBIT.

The visible spectrometer is also installed. The pinhole camera is used to monitor the electron beam shape, which is important for evaluating the EBIT performance and also for determining the absolute electron density. The characteristics of the spectrometers are also listed in TABLE 1.

TABLE 1. Specification of CoBIT apparatuses.

	Compact EBIT (CoBIT)	
Electron energy (keV)	0.1~2	
Electron current (mA)	10	
Maximum magnetic field (T)	0.2	
Coolant	LN_2	
EUV spectrometer (grating)	30-002 (Shimadzu)	30-001 (Shimadzu)
Groove number (l/mm)	1200	2400
Incident angle (degree)	87	88.65
Incident distance (mm)	237	237
Useful wavelength range (nm)	5-20	1-6
CCD detector	PIXIS-XO:400B, Princeton Instruments	

3.Results and discussion

FIGURE 2 shows EUV spectra obtained by using CoBIT with electron energies between 490 and 1440 eV. The corrections for the spectrometer response and the detector efficiencies were applied to the spectra shown in this figure. It is clear from the figure that the overall EUV spectra show significant dependence on the electron energy. The two peaks denoted by A and B are considered to be the emissions from the maximum charge state ion at each electron energy because they were not seen in the spectra with lower electron energies. For example, when the electron energy E_e increases from 620 to 670 eV, the maximum tungsten ion charge q produced in CoBIT is increased from 22+ to 23+. The emission lines of W XXII, which could not been seen at E_e= 620 eV, were observed at 27Å (Peak A) and 34Å (Peak B) at E_e =670 eV. As electron energy increases from 490 to 1440 eV, the charge states of the ions emitting these lines vary from W XIX to W XXXIII (W^{20+} ~ W^{34+}). In each spectrum, the emission lines from three or four charge states of highly charged tungsten ions are observed simultaneously. As the charge state increases, wavelengths of these emission lines (Peaks A and B) shift to the shorter wavelength-region.

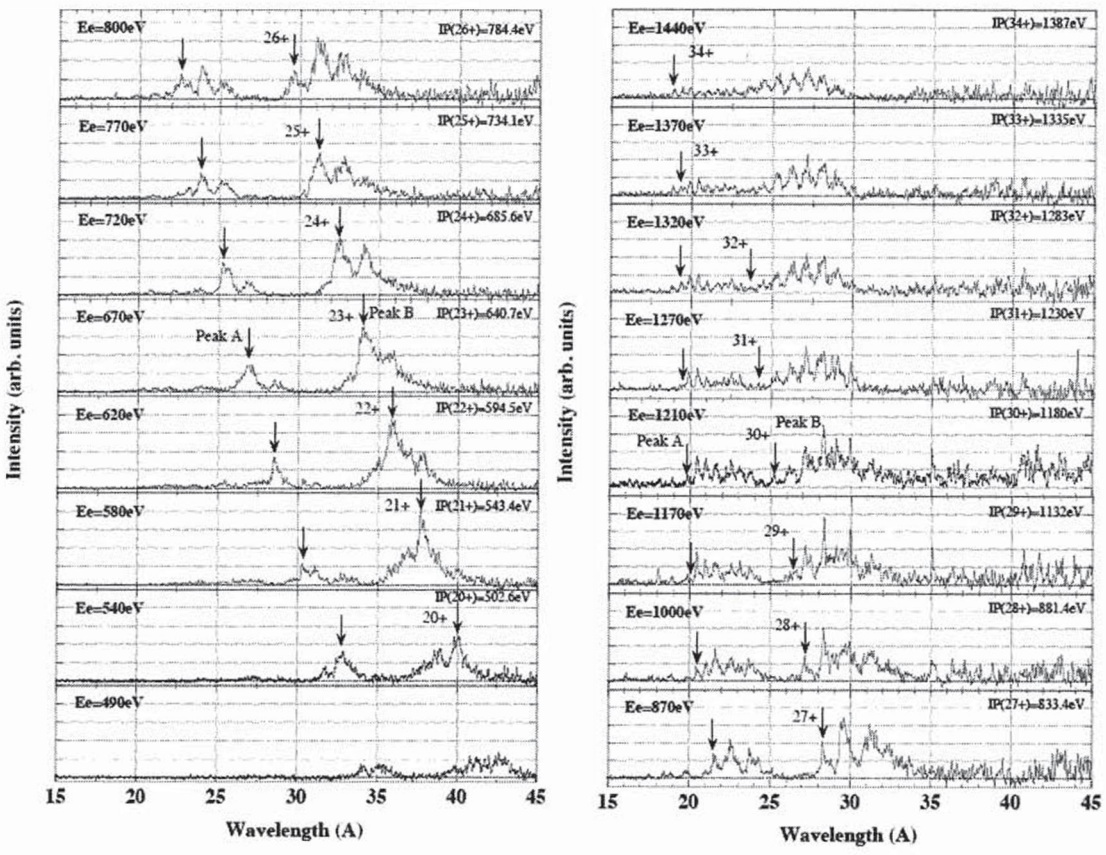

FIGURE 2. Typical EUV spectra of highly charged tungsten ions obtained at electron energy *Ee* from 490eV to 1440eV in CoBIT. *IP(q+)* is the *qth* ionization energy of tungsten ion.

FIGURE 3 shows the charge state dependence of the wavelengths for the peaks A and B. Circles and triangles are the experimental values for the peaks A and B, respectively. The solid line, dotted line and dash-dot line are the calculated wavelength corresponding to the 5f-4d, 5g-4f and 6g-4f transition manifolds, respectively. The calculated wavelength was obtained by averaging the wavelengths of all the transitions in each manifold weighted by the line strengths, which were calculated in an originally developed collisional-radiative model using atom data which were calculated by using the HULLAC code[12] in so-called configuration mode. In the configuration mode, each energy level is not calculated, and only a configuration averaged energy of a given configuration and a total angular momentum J is concerned. Therefore, the configuration interaction is not considered in this calculation. The charge dependence of peak B agrees with that of the 5g-4f transition.

The experimental value of peak A agrees with that of the 6g-4f transition for the charge state of the tungsten ions lower than 28+. When the charge state becomes higher than 28+, the wavelength of peak A appears corresponding to that of the 5f-4d transition. When the charge state of the tungsten ions is lower than 28+, since the 4d-shell is closed in the ground state and the 4f-shell becomes the valence-shell, the 5f-4d excitation is an inner-shell excitation process. Probably, the 5f-4d radiative transition has a smaller branching ratio to the Auger processes; the emission line thus disappears for the lower charge states. Since it happens that the wavelength of the 6g-4f transition gets close to that of the 5f- 4d transition at the charge states of 27- 28+, the measured wavelength curve of Peak A appears to transfer to that of 6g-4f transition at these charges states.

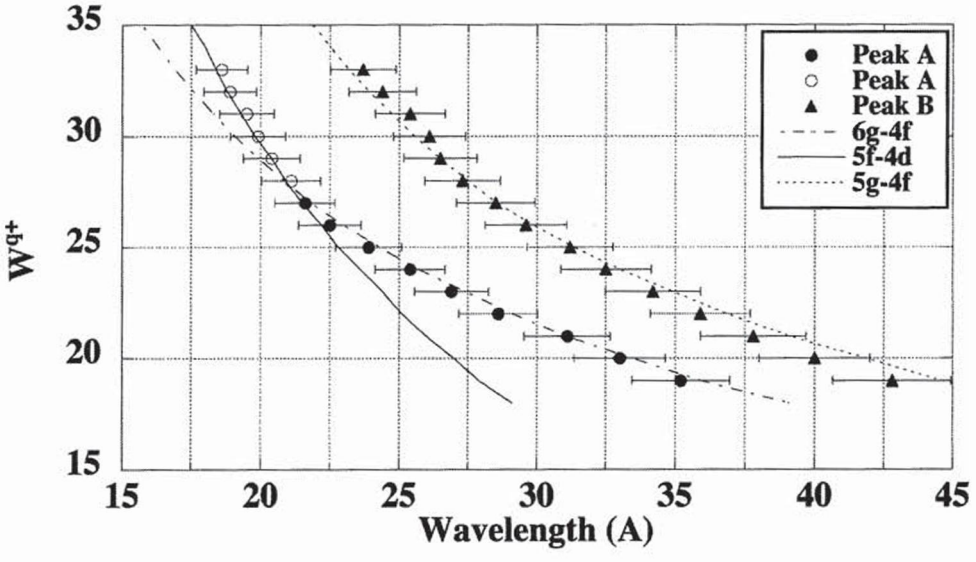

FIGURE 3. The wavelength shift of EUV emission lines

Acknowledgements

This work was partly supported by the JSPS-NRF-NSFC A3 Foresight Program in the field of Plasma Physics (NSFC: No.11261140328), the NIFS Collaboration Research program (NIFS10KOAJ003) and Grant-in-Aid for Scientific Research (A) (23246165) and (B) (22340175).

References

1. T. Pütterich *et al.*, J. Phys. B **38**, 3071 (2005).
2. M. B. Chowdhuri *et al.*, Plasma and Fusion Research **2**, S1060 (2007).
3. J. Clementson and P. Beiersdorfer, J. Phys. B **43**, 144009 (2010).
4. J. Clementson and P. Beiersdorfer, Phys. Rev. A **81**, 052509 (2010).
5. Y. Ralchenko *et al.*, J. Phys. B **40**, 3861 (2007).
6. S.Wu and R. Hutton, Can. J. Phys. **86**, 125 (2008)
7. Y.Podpaly *et al.*, Phys. Rev. A **80**, 052504 (2009)
8. N. Nakamura *et al.*, Phys. Scr. **T73**, 362 (1997).
9. N. Nakamura *et al.*, Rev. Sci. Instrum. **79**, 063104 (2008).
10. H. A. Sakaue *et al.*, J. Phys.:Conf. Ser. **163**, 012020 (2009).
11. H. Ohashi *et al.*, Rev. Sci. Instrum. (2011) in press.
12. A. Bar-Shalom, M. Klapisch, and J. Oreg, J. Quant. Spectr. Rad. Transf. **71**, 179 (2001)